Journal of Alloys and Compounds 862 (2021) 158442

Contents lists available at ScienceDirect

Journal of Alloys and Compounds

journal homepage: www.elsevier.com/locate/jalcom

Structure, electronic and optical properties of $CsPbX_3$ halide perovskite: A first-principles study

Han Chen[a], Minghao Li[a], Bin Wang[b], Sen Ming[a], Jing Su[a,*]

[a] School of Physics and Optoelectronic Engineering, Nanjing University of Information Science & Technology, Nanjing 210044, China
[b] School of Chemical, Biological and Materials Engineering, University of Oklahoma, Norman, OK 73019, USA

ARTICLE INFO

Article history:
Received 25 November 2020
Accepted 19 December 2020
Available online 30 December 2020

Keywords:
Perovskite
First principles
Photoelectric properties
Band structure
Density of states
Absorption spectrum

ABSTRACT

$CsPbX_3$ (X = halide) perovskites have promising optoelectronic application in solar cells, light-emitting diodes, and photodetection. Here, we report the atomic structure, electronic and optical properties of $CsPbX_3$ (X = I, Br, Cl, mixed-halide) using density functional theory calculations. The structure of $CsPbX_3$ changes with the change of halide ratio. All the $CsPbX_3$ compounds are direct bandgap semiconductors, and their valence band maximum is dominated by halide p orbitals, hybridizing with Pb 6s orbitals. With the gradually increasing of the lattice volume of the $CsPbX_3$ primary cell, the corresponding band gap value decreases accordingly, and the absorption spectra are red-shifted. The carrier mobility performance is estimated by the effective mass calculation, showing feasible charge transport properties. By adjusting the halide ratio, $CsPbX_3$ (X = I, Br, Cl, mixed-halide) possess the tunable band gap in the whole visible light range, which is of great significance for the development of new-type, high-efficient semiconductor materials and optoelectronic devices.

© 2020 Elsevier B.V. All rights reserved.

1. Introduction

In recent years, organic-inorganic halide perovskites have attracted much attention in the field of optoelectronics due to their excellent optical absorption, good carrier mobility, and long carrier lifetime [1]. Since the first organic-inorganic halide perovskite-based solar cell was reported, the power conversion efficiency (PCE) of the organic-inorganic hybrid halide perovskite-based solar cell has rapidly increased from 3.81% to 25.2% within a few years [2–8]. Most of these solar cells with a high power conversion efficiency adopt organic cations, such as methyl ammonium(MA) and formamidinium (FA). Though they have high PCE, due to the volatility of organic components and their poor thermal stability at high temperatures, their commercial application has many limitations.

To solve the problem of poor stability of organic-inorganic hybrid perovskite materials $CH_3NH_3PbX_3$, extensive researches have been focused on all-inorganic perovskite materials. By replacing the MA^+ with cesium ion, a series of new-type all-inorganic materials have been reported. In 2013, Stoumpos et al. successfully prepared $CsPbBr_3$ crystals by mixing equimolar solutions of $PbBr_2$ and CsBr in concentrated aqueous hydrobromic acid or by reacting equimolar amounts of CsBr and $PbBr_2$ in a sealed fused silica ampule at 600 °C, respectively. The experimental results have shown that $CsPbBr_3$ is a direct band gap semiconductor with an energy band gap of 2.25 eV at room temperature [9]. At the same time, $CsPbBr_3$ also shows high attenuation, high resistivity and significant photoconductivity response, indicating its broad application prospects in the field of photoelectric detection, and would be used for efficient and stable solar cells. Recently, Huang et al. prepared γ-$CsPbI_3$ films, in which a small amount of H_2O was added to the $CsPbI_3$ precursor solution to tune the equilibrium of the proton transfer process. The PCE effect of the γ-$CsPbI_3$ film with ideal electronic structure and photoelectric properties has reached 11.3% [10]. Mix-halide $CsPbX_3$ compounds, such as $CsPbIBr_2$ [11] and $CsPbI_2Br$ [12] perovskite solar cells have been reported by Baillie et al. and Liu et al., respectively, and the latter showed an efficiency of 15.56% and an open circuit voltage of 1.30 V. Additionally, ytterbium-doped $CsPbBr_{1.5}Cl_{1.5}$ perovskite quantum dots have realized nearly 90% photoluminescence quantum yield (PLQY) in near-infrared range [13]. Considering there is few systematic reports on the basic properties of the $CsPbX_3$ (X = I, Br, Cl, mixed-halide) compounds, here we report the structure stability, electrical and optical properties of 10 types of $CsPbX_3$ compounds. In our calculation, the influence of the spin-orbit coupling (SOC) effect on the band gap with different ratios of halide ions has been explored. The calculated electronic structure and absorption spectra suggest tunable absorption within the range of visible lights and

* Corresponding author.
E-mail address: sj007@nuist.edu.cn (J. Su).

https://doi.org/10.1016/j.jallcom.2020.158442
0925-8388/© 2020 Elsevier B.V. All rights reserved.

feasible charge transport properties. Our work is thus valuable for exploring the potential application of $CsPbX_3$ perovskite materials in optoelectronic devices, such as solar cells, light-emitting diodes, photoelectric detection, etc.

2. Theoretical calculations

The calculations of crystal structures, electronic and optical properties were performed using density functional theory (DFT) as implemented in the Vienna Ab-initio Simulation Package (VASP) [14]. The generalized gradient approximation was employed using the exchange and correlation function of Perdew, Burke, and Ernzerhof (GGA-PBE) [15]. In the calculation, the plane-wave cutoff energy was set to 400 eV. The atomic structures were optimized using the PBE functional with 9 × 9 × 9 Monkhorst-Pack k-point grid. For structural optimization and self-consistent convergence calculation, the energy convergence criterion of the system was set to 10^{-6} eV, and the force criterion was set to 0.02 eV/Å. The electronic and optical properties were calculated using the PBE and hybrid exchange-correlation functional (HSE06) [16], respectively with a cutoff energy of 400 eV. Due to the strong relativistic effect of Pb, the perovskite materials often show spin-orbit coupling effect (SOC) [17]. The band structures with considering the SOC effect were additionally calculated for the compounds of $CsPbCl_3$ and $CsPbBr_3$.

3. Results and discussion

3.1. Structural properties

Generally, the structural stability of perovskite ABX_3 compounds can be estimated by the Goldschmidt tolerance factor $t = \frac{R_A + R_X}{\sqrt{2} \cdot (R_B + R_X)}$ [18] and the octahedral factor $\mu = \frac{R_B}{R_A}$ [19]. A stable three-dimensional halide perovskite structure can usually be formed at $0.80 \le t \le 1.0$ and $0.44 \le \mu \le 0.9$. For $CsPbX_3$ (X = Cl, Br, I) and mixed-halide $CsPbX_3$, the $\mu = 0.71$ and the t values are in the range of (0.817–0.91), indicating a stable perovskite structure. At room temperature, $CsPbX_3$ is cubic crystal and the space group is $Pm\bar{3}m$. When there are two kinds of halide ions in $CsPbX_3$ with an ratio of 1:2, the space group changes to $P4mmm$; when there are three kinds of halogen ions in $CsPbX_3$ with the halide ratio of 1:1:1, the crystal structure changes to $Pmmm$. Taking the crystal structures of $CsPbI_3$, $CsPbBr_2Cl$ and CsPbIBrCl as examples, the three crystal structures are shown in Fig. 1.

Table 1 shows the crystal structure, calculated lattice constants and band gap values of the $CsPbX_3$ compounds, and Table S3 shows the bond lengths of the Pb-X. From I to Cl, the primary cell volume, the bond length is decreased when more X ions with smaller ionic radius are incorporated in the lattice.

Fig. 2 shows the relationship between the primary cell volume of $CsPbX_3$ compounds and the band gap Eg. The reported experimental value Eg of $CsPbBr_3$ crystal is 2.25 eV [9], which is quite close to our HSE result. Regardless of the PBE or the HSE functionals applied in the calculations, the Eg value increases as the cell volume decreases. By adjusting the ratio of halide ions, the crystal structure is changed and the band gap is tuned in the entire visible light region.

3.2. Electronic properties

Fig. 3 shows the band structures of single halogen $CsPbX_3$ crystal and some mixed-halide crystal using the PBE function. It can be seen from the energy band graph that both the valence band maximum (VBM) and the conduction band minimum (CBM) are located at point R in the reciprocal space (Kx = Ky = Kz = π/a), showing that all these compounds are direct band gap semiconductors. The calculated energy band gap value of $CsPbI_3$ is 1.48 eV, which is close to the ideal optical bandgap (1.34 eV) [22] required by single-junction solar cells, indicating that the material has a good potential application prospect in solar cells. In addition, as the lattice decreases, VBM decreases and CBM increases, and thus the Eg gradually increases, as shown in Table 1 and Fig. 2. For the compounds with higher Eg value, such as $CsPbBrCl_2$, and $CsPbCl_3$, would have potential application in photoelectric detection fields.

Considering the similarity of the electronic properties of the mixed-halide perovskite $CsPbX_3$, we also showed the total density of states (TDOS) of the $CsPbX_3$ crystal near the Fermi level and the partial density of states (PDOS) of some mixed-halide crystals in Fig. 4. The changing trend of Eg value with lattice, as derived from the DOS calculations, is consistent with the results from band structure analysis.

For the single-halide $CsPbX_3$ compounds, taking $CsPbBr_3$ as an example, it can be seen from Fig. 4(b) that the top of the valence band of $CsPbBr_3$ is mainly contributed by the anti-bonding hybrid

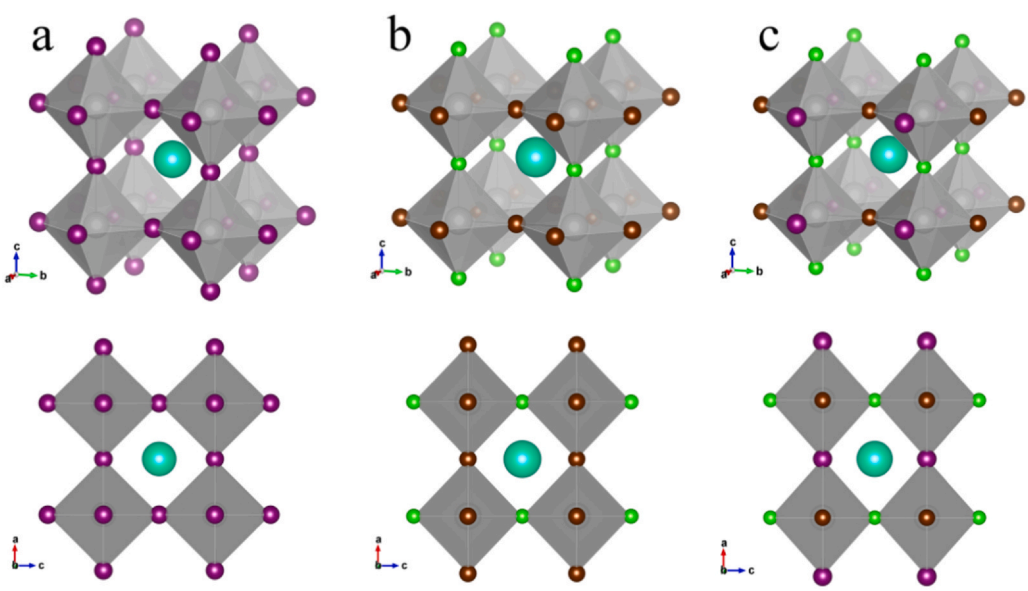

Fig. 1. The crystal structure of $CsPbI_3$, $CsPbBr_2Cl$ and CsPbIBrCl and their corresponding top view, (a) $CsPbI_3$, (b) $CsPbBr_2Cl$, (c) CsPbIBrCl, the difference of each atom lies in the color, Cs: cyan, Pb: gray, I: purple, Br: brown, Cl: green.

Table 1
The structure information and energy gap value Eg of $CsPbX_3$.

Sample	Space group	Lattice parameter	Primary cell volume (Å^3)	Primary cell energy (eV)	PBE-E_g (eV)	HSE-E_g (eV)
$CsPbI_3$	$Pm\bar{3}m$	a = b = c = 6.39266	261.24	-19.66	1.48	2.02
$CsPbI_2Br$	$P4/mmm$	a = b= 6.40655 c = 5.96181	244.70	-16.37	1.49	2.11
$CsPbI_2Cl$	$P4/mmm$	a = b = 6.42334 c = 5.68033	234.37	-16.91	1.52	2.17
$CsPbIBr_2$	$P4/mmm$	a = b = 5.98832 c = 6.40540	229.70	-16.98	1.53	2.19
CsPbIBrCl	$Pmmm$	a = 6.41811 b = 6.01217 c = 5.70050	219.96	-17.52	1.57	2.19
$CsPbICl_2$	$P4/mmm$	a = b= 5.72510 c = 6.41646	210.31	-18.05	1.62	2.31
$CsPbBr_3$	$Pm\bar{3}m$	a = b = c = 5.98372	214.25	-17.64	1.75	2.47
$CsPbBr_2Cl$	$P4/mmm$	a =b = 6.00178 c = 5.70393	205.46	-18.17	1.81	2.54
$CsPbBrCl_2$	$P4/mmm$	a = b = 5.71048 c = 6.01108	196.02	-18.73	1.85	2.62
$CsPbCl_3$	$Pm\bar{3}m$	a = b = c = 5.70687	185.86	-19.32	2.16	2.94

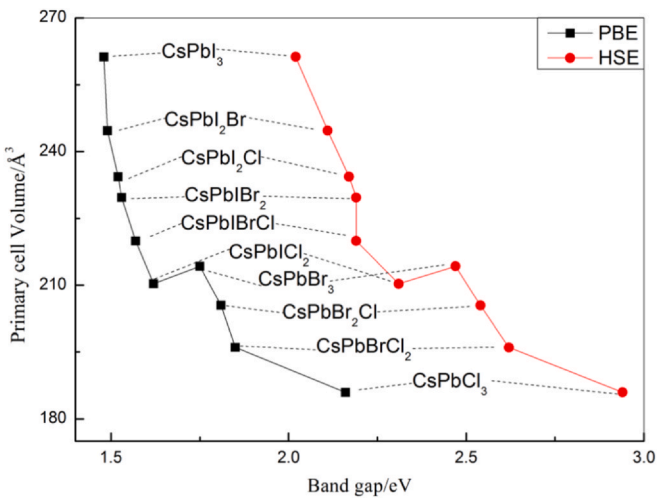

Fig. 2. The relationship between the compound cell volume and Eg of $CsPbX_3$.

state of Br-4p and Pb-6s, and the bottom of the conduction band is mainly Pb-6p state. For the mixed-halide $CsPbX_3$ crystals, taking $CsPbI_2Br$ and CsPbIBrCl as examples, Fig. 4(c) and (d) show that the valence bands of $CsPbI_2Br$ and CsPbIBrCl are mainly contributed by halide ions. The VBM of $CsPbI_2Br$ is composed of I-5p, Br-4p states, hybridizing with a small amount of Pb-6s. The VBM of CsPbIBrCl is composed of I-5p, Br-4p, Cl-3p orbitals, and a small amount of Pb-6s orbitals, and the energy levels of I-5p state are higher than Br-4p and Cl-3p states; the CBM of $CsPbI_2Br$ and CsPbIBrCl is mainly composed of Pb-6p state. When electrons are excited by light, it will transition from the anti-bonding orbital hybridized by I-5p, Br-4p/In-5p, Br-4p, Cl-3p and Pb-6s to the Pb-6p orbital. There is no obvious DOS of Cs^+ near the Fermi level, indicating the probability of electron transition of Cs^+ is very small and the main function of Cs^+ is to maintain the stability of the perovskite structure, by providing charge balance for PbX_3 framework.

Table 2 and Table S2 list the effective mass of electrons and holes along the path X(0, 0.5, 0) → R(0, 0.5, 0.5) for some $CsPbX_3$ compounds. As is shown in the Table 2, the carriers' effective masses are relatively small, in the range of 0.34 m_0 - 0.44 m_0 for electrons and 0.24 m_0 - 0.26 m_0 for holes, suitable for charge transport. In general, the difference of carriers' effective mass between each compound is not great; with the radius of the halide ion decreases, it gradually decreases.

To further study the electrical properties of the $CsPbX_3$ compounds, the Bader charge values of each compound were calculated, as shown in Table S1. The Bader charge values of Cs^+ and PbX_3 are

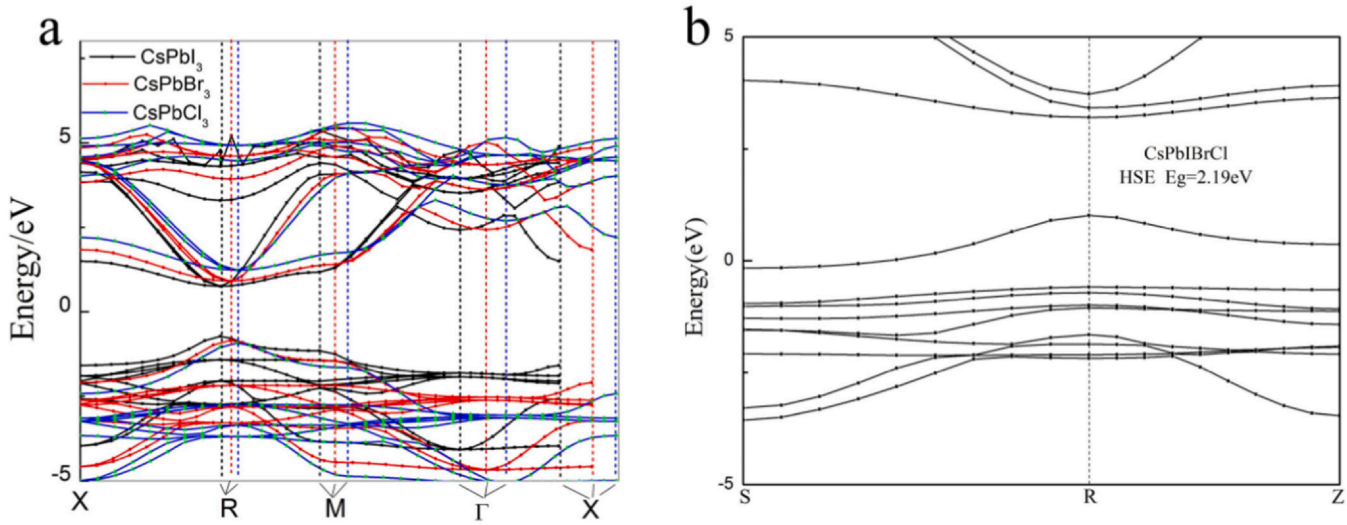

Fig. 3. Energy band structures of the single halogen $CsPbX_3$ and CsPbIBrCl compounds;(a) $CsPbX_3$ (X = Cl, Br, I), by PBE method; (b) CsPbIBrCl, by HSE method.

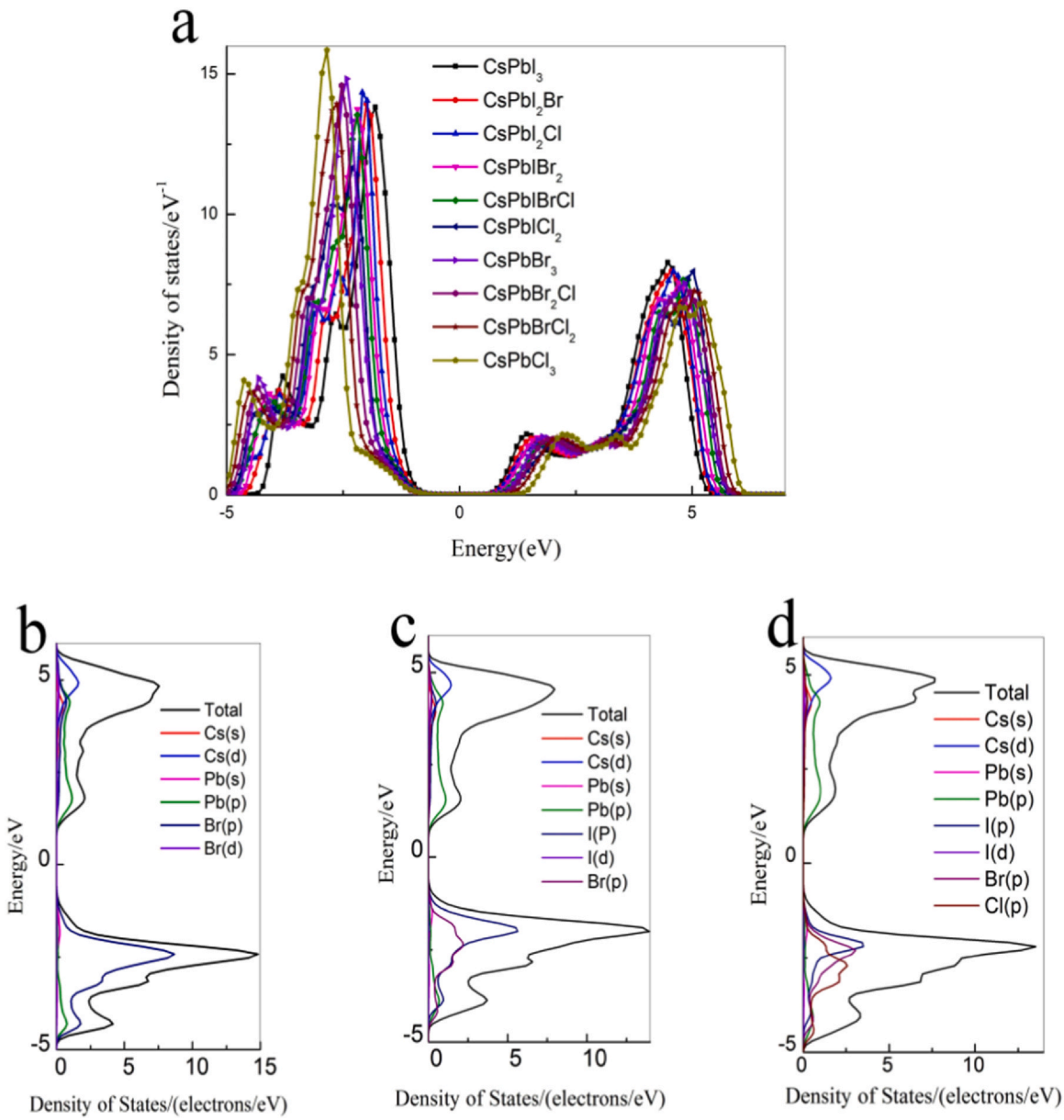

Fig. 4. (a) Total density of states (TDOS) of $CsPbX_3$ crystal; partial density of states (PDOS) of partially mixed halogens, (b) $CsPbBr_3$, (c) $CsPbI_2Br$, (d) CsPbIBrCl.

Table 2
Electron hole effective mass of $CsPbX_3$.

Compound	$CsPbI_3$	$CsPbIBr_2$	CsPbIBrCl	$CsPbBr_3$	$CsPbBr_2Cl$
$m_e(m_0)$	0.43	0.39	0.34	0.38	0.37
$m_h(m_0)$	0.26	0.24	0.26	0.24	0.24

relatively stable in all cases, about 0.87e - 0.88e, while it is much different for different halide ion. For the single halide $CsPbX_3$ compounds, from I to Br to Cl, the Bader charge of halide is accordingly increased, due to the increasing of the electronegativity of the halide ion. Table 3 listed the Bader charge of the $CsPbX_3$ (X = I, Cl, IBr, ICl) compounds. The Bader charge value of Cl ion (−0.63e) in $CsPbCl_3$ is much higher than that of I (−0.52e) in $CsPbI_3$; for the mix-halide compounds, the Bader charge value of I ion (−0.55e) is smaller than of Br ion (−0.66e) in $CsPbIBr_2$, and it is also the same in $CsPbICl_2$, indicating that the Bader charge is greatly related to the electronegativity of halide ion, as expected.

Due to the strong relativistic effect of Pb, we calculated the band structures of $CsPbX_3$ with considering the spin-orbit coupling (SOC) effect. As shown in Fig. 5, the band structures of $CsPbCl_3$ and $CsPbBr_3$ with and without SOC consideration are much different. The Eg values of $CsPbCl_3$ and $CsPbBr_3$ with the SOC effect taken into account in PBE calculations are reduced from 2.16 eV and 1.75–1.06 and 0.66 eV, respectively, by nearly 1.1 eV in both cases, indicating the

Table 3
The charge distribution of $CsPbCl_3$, $CsPbI_3$, $CsPbICl_2$ and $CsPbIBr_2$.

$CsPbCl_3$					
Element	Cs	$PbCl_3$	Pb	Cl	
Bader charges	0.879	-0.879	1.002	-0.627	
$CsPbI_3$					
Element	Cs	PbI_3	Pb	I	
Bader charges	0.870	-0.870	0.705	-0.525	
$CsPbIBr_2$					
Element	Cs	$PbIBr_2$	Pb	I	Br
Bader charges	0.871	-0.871	0.988	-0.546	-0.656
$CsPbICl_2$					
Element	Cs	$PbICl_2$	Pb	Cl	I
Bader charges	0.870	-0.870	0.988	-0.624	-0.609

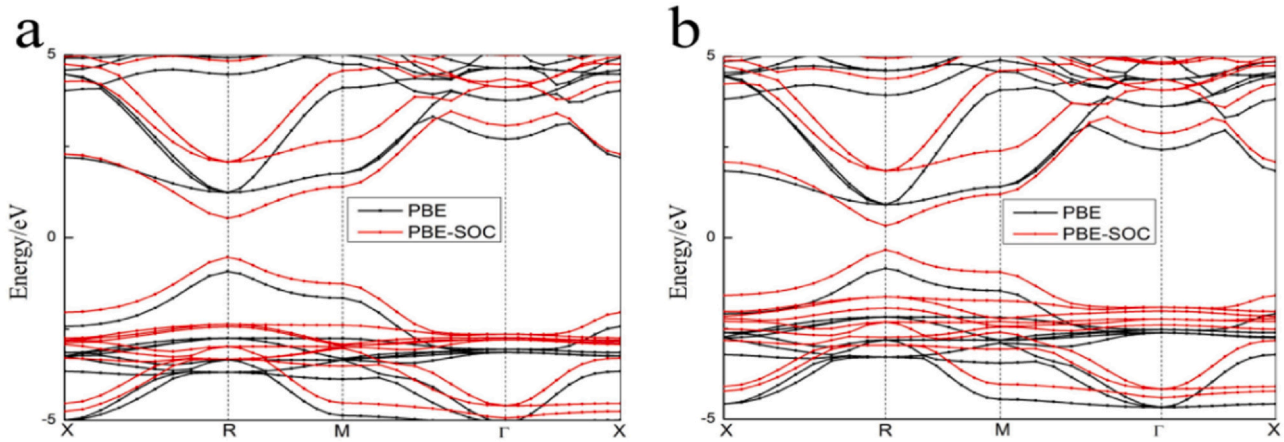

Fig. 5. The energy band structure of the $CsPbCl_3$(a) and $CsPbBr_3$(b) compounds near the Fermi level [−5 eV, 5 eV] calculated using the PBE function with and without considering the SOC effect.

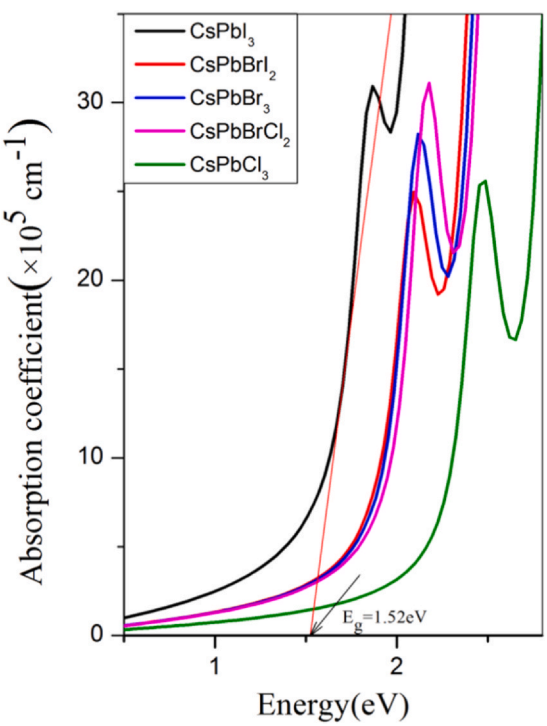

Fig. 6. Absorption spectra of the $CsPbX_3$ perovskite compounds.

influence of SOC on the energy band structure of $CsPbCl_3$ and $CsPbBr_3$ is significant and almost the same in $CsPbX_3$.

3.3. Spectral properties

Fig. 6 shows the absorption spectra of some single halide and mixed-halide $CsPbX_3$ perovskites. The absorption coefficient of perovskite is obtained from the real and imaginary parts of the dielectric function. The specific calculation formula α(ω) is as follows [20]:

$$\alpha(\omega) = \frac{\sqrt{2}e}{\hbar c}\left[\left(\varepsilon_1^2 + \varepsilon_2^2\right)^{1/2} - \varepsilon_1\right]^{1/2}$$

where $\varepsilon_1(\omega)$ and $\varepsilon_2(\omega)$ are the real and imaginary parts of the dielectric function, respectively, and ω is the photon frequency [21].

It shows that in the visible optical range, the absorption optical intensity of $CsPbX_3$ shows an overall upward trend as the energy increases, and the absorption spectrum red shifts with the increase of the lattice of $CsPbX_3$ crystal. Among these materials, $CsPbI_3$ has better absorption characteristics, and its absorption edge of $CsPbI_3$ is located at 1.52 eV, indicating that $CsPbI_3$ would absorb all-range of visible light and has great potential as a photoelectric conversion material for perovskite solar cells. For the $CsPbX_3$ material with a larger band gap, it is expected to be applied in optoelectronic devices, such as photodiodes, photo detectors, etc.

4. Conclusions

In conclusion, the crystal structure, energy band structure, electrical properties and optical absorption properties of $CsPbX_3$(X = I, Br, Cl, mixed halide) perovskites were calculated. The results showed that these $CsPbX_3$ compounds are direct band gap semiconductors; with more halide ion of larger ion radius incorporated into the lattice, the lattice volume of perovskite $CsPbX_3$ gradually increases. With the lattice increases, the energy of the VBM is increased and CBM is decreased accordingly, and the corresponding band gap value gradually decreases. The Bader charge is related to the electronegativity of the halide element, which increases from I to Br to Cl. The absorption spectra of $CsPbX_3$ compounds are red-shifted with the increasing of halide ions of larger sizes, and the absorption optical intensity in the visible optical region shows an increasing trend. The calculation results show that, by changing the halide ratio, the band gap can be tuned in the visible optical region, which is expected to have important application prospects in solar cells, light-emitting diodes, photodetectors, and so on.

Declaration of Competing Interest

The authors declare that they have no known competing financial interests or personal relationships that could have appeared to influence the work reported in this paper.

Acknowledgments

This work is supported by the National Natural Science Foundation of China (No. 51472123).

Appendix A. Supporting information

Supplementary data associated with this article can be found in the online version at doi:10.1016/j.jallcom.2020.158442.

References

[1] M.A. Green, A. Ho-Baillie, H.J. Snaith, The emergence of perovskite solar cells, Nat. Photonics 8 (2014) 506–514.

[2] W.S. Yang, B.W. Park, E.H. Jung, N.J. Jeon, Y.C. Kim, D.U. Lee, S.S. Shin, J. Seo, E.K. Kim, J.H. Noh, S.I. Seok, Iodide management in formamidinium-lead-halide-based perovskite layers for efficient solar cells, Science 356 (6345) (2017) 1376–1379.

[3] H.S. Kim, C.R. Lee, J.H. Im, K.B. Lee, T. Moehl, A. Marchioro, S.J. Moon, R. Humphry-Baker, J.H. Yum, J.E. Moser, M. Grätzel, N.G. Park, Lead iodide perovskite sensitized all-solid-state submicron thin film mesoscopic solar cell with efficiency exceeding 9%, Sci. Rep. 2 (2012) 1–7.

[4] M. Saliba, T. Matsui, J.Y. Seo, K. Domanski, J.P. Correa-Baena, M.K. Nazeeruddin, S.M. Zakeeruddin, W. Tress, A. Abate, A. Hagfeldt, M. Grätzel, Cesium-containing triple cation perovskite solar cells: improved stability, reproducibility and high efficiency, Energy Environ. Sci. 9 (6) (2016) 1989–1997.

[5] W.S. Yang, J.H. Noh, N.J. Jeon, Y.C. Kim, S. Ryu, J. Seo, S.I. Seok, High-performance photovoltaic perovskite layers fabricated through intramolecular exchange, Science 348 (6240) (2015) 1234–1237.

[6] M.K. Nazeeruddin, H. Snaith, Methylammonium lead triiodide perovskite solar cells: a new paradigm in photovoltaics, MRS Bull. 40 (08) (2015) 641–645.

[7] A. Kojima, K. Teshima, Y. Shirai, T. Miyasaka, Organometal halide perovskites as visible-light sensitizers for photovoltaic cells, J. Am. Chem. Soc. 131 (17) (2009) 6050–6051.

[8] G.E. Eperon, S.D. Stranks, C. Menelaou, M.B. Johnston, L.M. Herz, H.J. Snaith, Formamidinium lead trihalide: a broadly tunable perovskite for efficient planar heterojunction solar cells, Energy Environ. Sci. 7 (3) (2014) 982–988.

[9] C.C. Stoumpos, C.D. Malliakas, J.A. Peters, Z. Liu, M. Sebastian, J. Im, T.C. Chasapis, A.C. Wibowo, D.Y. Chung, A.J. Freeman, B.W. Wessels, M.G. Kanatzidis, Crystal growth of the perovskite semiconductor $CsPbBr_3$: a new material for high-energy radiation detection, Cryst. Growth Des. 13 (7) (2013) 2722–2727.

[10] B. Zhao, S.F. Jin, S. Huang, N. Liu, J.Y. Ma, D.J. Xue, Q. Han, J. Ding, Q.Q. Ge, Y. Feng, J.S. Hu, Thermodynamically stable orthorhombic γ-$CsPbI_3$ thin films for high-performance photovoltaics, J. Am. Chem. Soc. 140 (37) (2018) 11716–11725.

[11] M. Zhang, J.S. Yun, Q. Ma, J. Zheng, C. Lau, X. Deng, J. Kim, D. Kim, J. Seidel, M.A. Green, S. Huang, A. Ho-Baillie, High-efficiency rubidium-incorporated perovskite solar cells by gas quenching, ACS Energy Lett. 2 (2) (2017) 438–444.

[12] H. Zhao, Y. Han, Z. Xu, C. Duan, S. Yang, S. Yuan, Z. Yang, Z. Liu, S. Liu, A novel anion doping for stable $CsPbI_2Br$ perovskite solar cells with an efficiency of 15.56% and an open circuit voltage of 1.30 V, Adv. Energy Mater. 9 (40) (2019) 1902279.

[13] S.Y. Zhao, Y.B. Zhang, Z.G. Zang, Room-temperature doping of ytterbium into efficient nearinfrared emission $CsPbBr_{1.5}Cl_{1.5}$ perovskite quantum dots, Chem. Commun. 56 (2020) 5811–5814.

[14] G. Kresse, J. Furthmüller, Efficiency of ab-initio total energy calculations for metals and semiconductors using a plane-wave basis set, Comput. Mater. Sci. 6 (1) (1996) 15–50.

[15] J.P. Perdew, K. Burke, M. Ernzerhof, Generalized gradient approximation made simple, Phys. Rev. Lett. 77 (18) (1996) 3865–3868.

[16] J. Heyd, G.E. Scuseria, M. Ernzerhof, Hybrid functionals based on a screened coulomb potential, Chem. Phys. 118 (2003) 8207–8215.

[17] J. Even, L. Pedesseau, J.M. Jancu, C. Katan, Importance of spin-orbit coupling in hybrid organic/inorganic perovskites for photovoltaic applications, J. Phys. Chem. Lett. 4 (17) (2013) 2999–3005.

[18] V.M. Goldschmidt, Die gesetze der krystallochemie, Naturwissenschaften 14 (21) (1926) 477–485.

[19] C.H. Li, X.G. Lu, W.Z. Ding, L.M. Feng, Y.H. Gao, Z.M. Guo, Formability of ABX_3(X = F, Cl, Br, I) halide perovskites, Acta Crystallogr. 64 (6) (2010) 702–707.

[20] M.G. Ju, J. Dai, L. Ma, X.C. Zeng, Perovskite chalcogenides with optimal bandgap and desired optical absorption for photovoltaic devices, Adv. Energy Mater. 7 (18) (2017) 1700216.

[21] J. Yuan, B. Gao, W. Wang, J. Wang, First-principles calculations of the electronic structure and optical properties of Y-Cu Co-doped ZnO, Acta Phys. Chim. Sin. 31 (7) (2015) 1302–1308.

[22] E. Meyer, D. Mutukwa, N. Zingwe, R. Taziwa, Lead-free halide double perovskites: a review of the structural, optical, and stability properties as well as their viability to replace lead halide perovskites, Metals 8 (9) (2018) 667–682.